

An Oscillation-based Algorithm for Reliable Vehicle Detection with Magnetic Sensors

Djamel Djenouri

CERIST Research Center
Algiers, Algeria
e-mail: ddjenouri@acm.org

Messaoud Doudou^{1,2} and Mohamed Amine Kafi^{1,2}

¹CERIST Research Center, Algiers, Algeria.

²USTHB, Algiers, Algeria.

e-mail: {doudou, kafi}@cerist.dz

Abstract—Vehicle monitoring using a wireless sensor network is considered in this paper, where a new algorithm is proposed for vehicle detection with magnetic sensors. The proposed algorithm is based on processing the magnetic signal and thoroughly analyzing the number/direction of its oscillations. The main feature of the proposed algorithm over the state-of-the-art ones is its capability to detect vehicles with different shapes of signatures, while most state-of-the-art algorithms assume regular shapes of signatures. This makes the algorithm effective with all types of magnetic sensors. The proposed algorithm has been implemented on MICAz sensor motes and tested in real world scenarios. Results show reliability beyond 93% in all samples, and more than 95% in most of them.

Keywords—wireless sensor networks; magnetic sensor; intelligent transport system

I. INTRODUCTION AND BACKGROUND

Existing road traffic surveillance and management technology may be divided into three categories [1], i) intrusive, ii) non-intrusive and iii) off-the-road. Most conventional systems use intrusive technologies, e.g., inductive loop detectors, micro-loop probes, pneumatic road tubes, piezoelectric cables, and weigh-in-motion sensors. Although featured with high accuracy for vehicle detection, this technology has many drawbacks such as the high cost, disruptions of traffic and infrastructure for installation and maintenance. This makes them inappropriate for large deployment in future road traffic surveillance systems. Non-intrusive technology is more appropriate for future deployments as it does not need any heavy installation on the carriageway and pavement, and their installation and maintenance do not cause disrupting of the traffic. Examples of this type of technology include microwave radar [2], cameras [3], wired infrared or ultrasonic sensors, passive acoustic array, and recently, wireless sensors. Off-roadway technology refers to the techniques that do not need any hardware to be setup under the pavement or on the roadside, such as GPS, mobile phones, remote sensing technology that makes use of images from aircrafts or satellites, etc. This technology is ad hoc and not self-sufficient, but they represent good candidates to complement non-intrusive technology. We are interested in this paper in the non-intrusive technologies, and particularly in the use of wireless magnetic sensors for vehicle detection, which represents a pillar to build any surveillance system. As vehicles have significant amounts of ferrous metals in their chassis (iron,

steel, nickel, cobalt, etc.), the magnetic field disturbance created by a vehicle is sufficient to be detected by a magnetic sensor [1]. This feature, added to the relatively high coverage area of magnetic sensors compared to line-of-sight sensors (infrared, ultra sonic, etc.), justifies the choice of this type of sensors in most systems [4]. While other line-of-sight sensors, e.g., ultra sonic, can be used in some limited applications such as car parks [5].

Kwon and Weidemann [6] use a wireless mesh network for the design of a vehicular tracking system that monitors vehicle movements at intersections. The wireless node of the network integrates an AMR (magnetic) sensor, along with PAN4570 radio for wireless communication. These nodes have been dug at the center of carriageways to detect disruption of the magnetic field caused by the passes of vehicles, and appropriate algorithms for detection, counting and tracking have been proposed. The algorithms are based on adaptive thresholds to determine the signal baselines¹, instead of static ones. The adaptation is made with the simple mobile average (SMA) method. A system for vehicle counting and speed estimation in highways and intersections has been proposed in [7]. HMC1051z sensors have been used along with Mica2dot motes. A WSN is configured to relay the collected information to an access point, then to the traffic management center. In their experiments with a sample of 333 vehicles, the authors report a precision of 97% for threshold based vehicle detection algorithm. Wang et al. [8] consider difficulties of the deployment of magnetic sensors on the roadside and the impact of the noise. They use the wavelets methods to filter the noise and improve accuracy of the magnetic signal. Experimental results demonstrated accuracy of 90.9%. Sifuentes *et al.* [4] propose the use of optical sensor as triggers to wake-up a magnetic sensor for the purpose of designing a power efficient detection system. All current systems use detection algorithms that rely on the regularity of magnetic signatures², i.e., they suppose the signature oscillations have the same shape. However, our experience revealed that regularity of the signatures is not satisfied for many magnetic sensors. For illustration, we investigated the signatures of more than 600 vehicles with HMC1002 magnetic sensor. Fig. 1 shows some signatures detected by the same sensor of different vehicles

¹ The interval for the values of the ambient magnetic field to be measured when there is no significant disruption, which changes over time.

² the signature here denotes the magnetic field variation over the time

moving at different speeds but towards the same direction. As illustrated, a vehicle pass may have a single positive oscillation, denoted OS+ (Fig. 1(a)), a negative one, denoted OS- (Fig. 1(b)), two oscillations of different orientations, Fig. 1(c) and Fig. 1(d) for respectively (OS+, OS-), (OS-, OS+), or (in very few occurrences) the same orientation Fig. 1(e), Fig. 1(f). A pass may also seldom result in three oscillations Fig. 1(g). Therefore, it is not possible to distinguish between a pass with more than a single oscillation from several continues passes with a single oscillation. All the existing solutions suppose regular signatures, i.e., two oscillations– (Os+,Os-) for one direction and (Os-,Os+) for the other– and thus they do not work for sensors with such irregular signatures. The contribution in this paper is to deal with this problem by proposing a new vehicle monitoring solution based on a detection algorithm that works for sensors with irregular signatures. Real world experimentation confirms the effectiveness of the proposed algorithm.

The rest of this paper is organized as follows: Section II gives a general overview of the proposed solution, and Section III presents in details the detection algorithm. Some experimentation results are reported in Section IV, and finally, the conclusion is drawn in Section V.

II. TYPE PROPOSED SOLUTION

The proposed solution for vehicle monitoring with networked wireless sensors uses magnetic sensors that should be deployed in the monitoring area (roundabout, entrance/exit to a city, a parking lot, etc.) to detect vehicle passes and report the collected data towards a base station, then a control center and/or Internet. We focus in this paper on the vehicle detection system that is composed of the following modules: i) sampling, ii) calibration, iii) filtering, iv) detection. Each of these modules is described in the following. Without loss of generality, HMC1002 magnetic sensor connected to MICAz mote, along with the TinyOS platform are used in the solution.

A. Sampling

It consists in acquiring the input magnetic signal from the sensor at a frequency that should be high enough to prevent the loss of any information related to vehicle pass. The hardware performs all the required signal processing on the continuous analogous magnetic signal, $S(t)$, to provide a digitalized discrete time signal, $E(t)$, as input to our system.

$E(t)$ can be read from the ADC of MICAz microcontroller with 10 bit signal resolution. The values of the HMC1002 output signal are within the interval, [200; 800], and they can be read at a sampling frequency to be set by the user through a software interface command. We have chosen 100Hz sampling frequency that corresponds to 10ms interval between two successive sample readings. This is high enough to theoretical detect signals from potential vehicles moving at a speed up to 150Km/h.

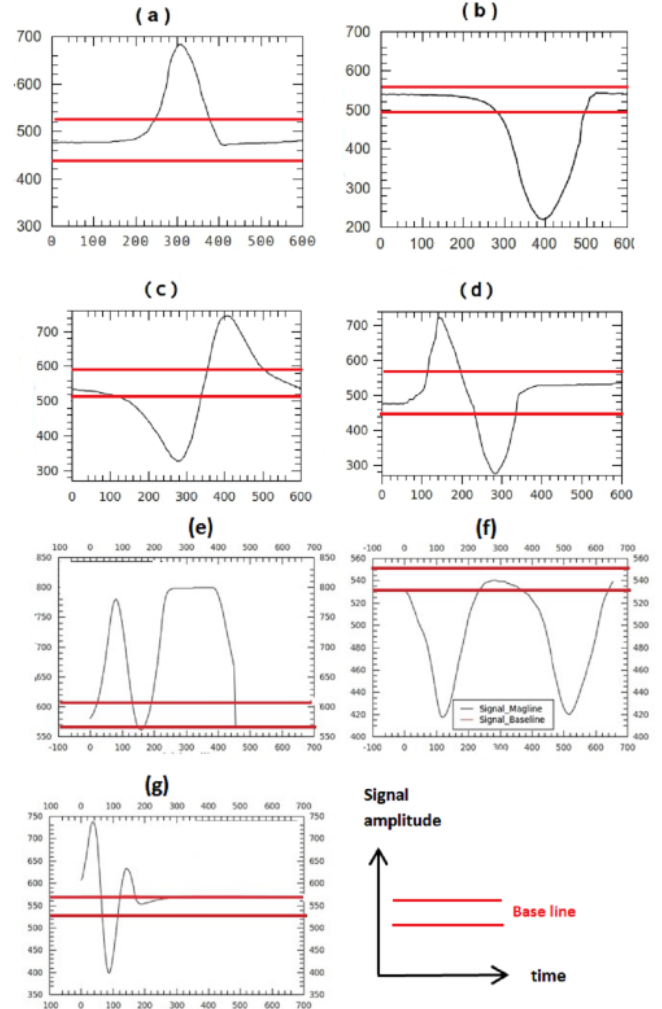


Figure 1. Different Types of Signatures

B. Filtering

Although the analogous signal $S(t)$ undergoes a preliminary filtering by the hardware before producing the digital signal $E(k)$, further application of numerical filters are required to eliminate high frequency noise. This step uses, $E(k)$, as input and produces on the output, $F(k)$, as a digital filtered signal. Given the limitations in computation and memory of sensor motes, infinite impulse response filter (IIR) has been chosen [9]. The filter has as input a set of N samples and provides a single recursive output, F . It is thus said to be of order, $(N,1)$, where the mean of N input samples is calculated and weighted with feedforward filter coefficient, $\alpha \in [0, 1]$, then added to a weighted value of the previous output, $F(k-1)$, using feedback filter coefficient, $\beta = \alpha - 1$. The following equation summarizes the chosen filter:

$$F(k) = \frac{\alpha \sum_{i=0}^{N-1} E(k-i)}{N} + \beta F(k-1) \quad (1)$$

In the detection algorithm presented later, IIR filters are calculated for both the detected magnetic signal, say $mag(k)$, and the ambient magnetic baseline, say $base(k)$.

C. Calibration

The magnetic signal interval, [200, 800], includes sensitivity interval, [300, 700], where the sensor is sensitive to magnetic field changes, and saturation interval (values out of the previous interval) where the sensor becomes saturated and unable to detect the perturbations of the magnetic field. The sensor is saturated at the startup, and may also be saturated after a long period of operation. Therefore, an algorithm that brings the signal to the sensitive interval is required, which is known as calibration. This is enabled by a potentiometer at the magnetic sensor, which accepts the injection of a low electrical pulse that alternates the internal magnetization of an internal vector. Once the vector is correctly aligned, the sensor is said to leave the saturation state and becomes sensitive. The potentiometer may be controlled via a software interface provided with the sensor driver. During the calibration phase, all the adjustment interval³ is scanned at the quest of a value that stabilizes the sensor and brings it into the sensitive interval. The process is repeated each time the sensor reports a value at the saturation interval. It can be summarized with this simple algorithm: i) initiate the adjustment variable, say at 0, ii) inject the variable through the potentiometer command interface, iii) increment the adjustment variable, iv) read the next sample and repeat steps (ii) to (iv) until reading a value within the sensitive interval.

III. DETECTION

A. Threshold Adaptation

Remember that the baseline represents the current value of the ambient magnetic field, but not all magnitude values beyond the baseline are due to vehicle presence. Small metallic objects may affect the sensor readings and thus a threshold should be defined to filter out readings due to small objects, which are not filtered by the previous filters. This threshold changes dynamically with the baseline. As the magnetic perturbation may have positive and negative oscillations (Fig. 1), two thresholds are used, $UpTh$ and $DownTh$, where $UpTh = base(k) + \delta$ and $DownTh = base(k) - \delta$. δ is a constant to be set empirically. As a result, only magnitude of signals beyond the thresholds (values of signals upper than $UpTh$ or lower than $DownTh$) are judged to be caused by vehicle presence.

B. Detection Algorithm

The detection algorithm is illustrated in Fig. 2. Three levels are defined: L^0 that represents readings between $UpTh$ and $DownTh$, L^+ for readings beyond $UpTh$, and L^- for readings below $DownTh$. A shifting vector, V , of size three is used, which represents previous readings. The vector shifts every time a reading at a level different from the current one

³ Interval of values accepted by the potentiometer, and which are used to bring the sensor into sensitivity state.

takes place. A counter, CO , is used to count the number of oscillations. Case 1 is the initial state, which also occurs after calibration or at the end of a signature during the period separating two passes of vehicles. Cases 2 and 8 represent the beginning of a signature (respectively with a positive and negative oscillation). Detection is reported by the mote when reaching these states. The report may have different forms depending on the application. For instance, it may consist in an instantaneous signaling for real-time surveillance applications, or increase of a counter and periodic signaling for counting-based applications (at intersections, entrances to a car parking or to some specific areas, etc.). Cases 3 and 6 represent the end of an oscillation (respectively a positive oscillation and negative oscillation). The oscillation can be the first one, or the second one of a single signature, which is identified using the counter CO that is incremented. The end of the second oscillation implicitly ends the detection by resetting CO to 0 and V_i to L^0 (to get $V_i = 0, \forall i \in \{0, 1, 2\}$), and then the system accordingly starts monitoring a new pass. However, the end of the first oscillation keeps the system in reading the same signature for a certain period before moving to a new one, which will be explained in the following. Cases 4 and 9 represent the beginning of an oscillation on the same direction as the previous one, i.e., a positive oscillation after a positive one (case 4), or a negative oscillation after a negative one (case 9). In this case, we consider that the previous signature includes a single oscillation and a new signature begins. The reason behind this assumption will be explained later. Cases 5 and 7 represent the beginning of an oscillation in the opposite direction of the previous one. The oscillation is then considered as the continuation of another one in a two oscillation signature. In addition to the actions represented in the table, additional actions are added. A timer is used to measure the duration when the signal remains at level, L^0 , after the first oscillation (cases 3 and 6 when $CO = 1$). After a timeout, the previous signature is considered to include a single oscillation and it is ended to allow the system to start monitoring of a new pass. This is by resetting CO to 0, and V_0 to L^0 . Note that cases corresponding to the beginning of an oscillation (cases 4, 5, 7, 9) take place only before the expiration of the timer. Otherwise, the beginning of the oscillation will correspond to cases 2 or 8. Another timer is used to account for the duration at the saturation state. After a timeout, the system runs the calibration algorithm and sets CO to 0, and V_i to $L^0, \forall i$.

C. Illustration

For illustration, let us consider a vehicle passe that generates the signature presented in Fig. 3. The signature is captured by a real sensor. Note that this represented the filtered signature, which is obtained by the sensor after applying the filtering algorithm presented above. Initially, after startup and calibration, the vector, V , is at state, $(L^0; L^0; L^0)$. At time $t1$ that corresponds to the first sample reading above $UpTh$, the vector shifts to $(L^0; L^0; L^+)$, and a detection is reported (case 2 of the table). At $t2$, it passes to $(L^0; L^+, L^0)$, and the counter CO is incremented to 1, then to $(L^+, L^0; L^-)$ and $(L^0; L^-, L^0)$, respectively at $t3$ and $t4$. CO will also be

incremented to reach 2. This represents the indication for the end of the second oscillation and ends the detection. V is reset to the initial state ($L^0; L^0; L^0$) and the sensor becomes again ready for new detection. Note that the times $t1; t2; t3; t4$ are as indication for the periods where the system changes its state, and they do not represent successive readings. In fact, many readings may take place during the period separating two times without causing any significant change, as long as the thresholds are not reached. The previous process is repeated for every pass of a vehicle. Signatures with one oscillation are detected with the same process, except that the end of the signature is determined with the expiration of the timer that counts the duration at L^0 when the system passes either the case 3 or case 6 and $CO = 1$ (the additional actions presented in the previous section).

Case	V_0	V_1	V_2	Action	Signal Form
1	L0	L0	L0	No action	
2	L0	L0	L+	Report a detection	
3	L0	L+	L0	CO = CO+1 if (CO = 2) CO = 0; V1 = L0 End if	
4	L+	L0	L+	Report a detection CO = 0	
5	L+	L0	L-	No action	
6	L0	L-	L0	CO = CO+1 if (CO = 2) CO = 0; V1 = L0 End if	
7	L-	L0	L+	No action	
8	L0	L0	L-	Report a detection	
9	L-	L0	L-	Report a detection CO = 0	

Figure 2. Different Cases of the Detection Algorithm

D. Limitations

Although the algorithm allows to reliably detect and identify many irregular signatures contrary to the state-of-the-art algorithms, it has some limitations. It cannot distinguish between, i) two successive single-oscillation signatures in the same direction, which may be caused by two vehicles that move very close to one another, and ii) a single signature with two oscillations on the same direction (Fig. 1(e) and (f)). As we empirically remarked that the former scenario is much more likely to happen than the second one, and that very few passes generate two oscillations in the same direction, the second oscillation is considered as the beginning of a new signature (cases 4 and 9 of the algorithm). Therefore, a pass of a vehicle with such a two-oscillation signature will be accounted twice and results in a false positive (in vehicle counting applications). A false positive also takes place for a signature with three oscillations (Fig. 1(g)) where the third oscillation will be considered as the beginning of a new signature. Such signatures happen very seldom, and the scenario of two passes causing similar sequence of oscillations is much more frequent. Finally, although the thresholds ($UpTh$ and

$DownTh$) are dynamically updated by the algorithm, a signature of oscillation(s) below the threshold may occasionally take place, which cannot be detected. The system will have a false negative in this case. The next section will empirically investigate the impact of such limitation on the overall effectiveness of the proposed algorithm. note that only counting-based applications are concerned with the false positive limitation, as the latter just causes duplicate notifications for tracking applications, and for other monitoring applications based on notification. however, false negatives (missing of detections) impact all applications.

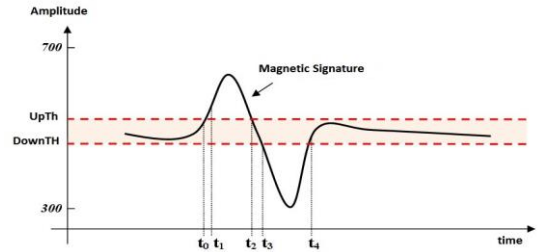


Figure 3. Illustrative Signature

IV. EXPERIMENTATION

The MTS310CA sensing board has been used to empower the mote with an HMC1002 magnetic sensor. Before evaluating the detection algorithm, we performed some preliminary tests to set intersect parameters of the algorithm such as the position of the sensor, the magnetic axe orientation, values of coefficients (α, β, δ), etc. The preliminary experiments at our campus show that putting the sensor on the carriageway is better than on the road side. However, it is impractical in the real world tests to have permission to dig the carriage way and put sensors just for experimentation; we thus considered the road side scenario. Results show a distance of 1.5 from the road side allows for effective detection/coverage and prevents fast saturation that is due to passe close to the road side. The coefficient α has been empirically set to $1/8$ for the magnetic field ($mag(k)$, Equation 1) and $1/64$ for the baseline ($base(k)$), then consequently β to $7/8$ and $63/64$ for $mag(k)$ and $base(k)$, respectively, while δ has been set to 15. We have also empirically improved the calibration algorithm by reducing its convergence time. The initial algorithm has a convergence time that may exceed $1sec$, which is extremely high. Instead of canonically increasing the potentiometer input value and scanning the whole interval, a search algorithm based on a divide and conquer method has been used. This improvement improves the calibration time and reduces it to less than $200ms$ in the worst case. This reduces false positives (non detections) due to periods of calibrations.

After the preliminary tests, the proposed algorithm has been tested in a real world scenario. With the help of our partner, the ministry of transportation, a crowded roundabout in the capital Algiers has been chosen. The roundabout is in a crossroad of a multi-lanes highway that narrows to a single lane at the intersection. This is an ideal scenario

for sensor deployment, and for getting meaningful samples in a short period of time (given the very high traffic at this area). Short period was needed as we used video sequences and manual off-line counting for ground truth. Five samples at different periods have been collected, analyzed, and the results are summarized in Table I. The table shows for every sample the real number of passing vehicles (say pv), i.e., the ground truth, the number of false positives (fp), and the number of false negatives (fn). False positives represent false detections that are due to duplicate detections. A duplicate detection takes place when a single vehicle pass with two oscillations in the same direction (or even with three oscillations in very few cases) is counted twice (Sec III-D). False negatives are the number of undetected vehicles, which are caused by passes that completely take place during calibration, or those generating a signal below the threshold. The fourth row represents the number of vehicles as detected by the system (say det), which is given by $det = pv + fp - fn$. The next row gives the percentage of correct counting (τ_c), defined by,

$$\tau_{c=1} = \frac{det - pv}{det} \quad (2)$$

The last row gives the percentage of successful detections, which is not affected by duplications but only false positives. It is defined by,

$$\tau_{d=1} = \frac{fp}{pv} \quad (3)$$

The results demonstrate the effectiveness of the algorithm, where the percentage of correct detections has been beyond 93% (and beyond 95% for all samples except the third). Moreover, for reliability in terms of counting the number of vehicles, where false negatives are compensated with false positives (which is typically tolerable in counting applications), the percentage is beyond 94% for the first sample, and even beyond 97% for all the others.

TABLE I. EXPERIMENTAL RESULTS

Sample	1	2	3	4	5
Passing vehicles	261	281	292	850	612
False positives	20	11	18	42	22
False negatives	6	8	19	16	21
Detection	275	284	291	876	613
Correct counting %	94.9	98.94	99.65	97.03	99.83
Correct detection %	97.70	96.08	93.83	95.05	96.40

V. CONCLUSION

Vehicle detection is the fundamental step for any road traffic Monitoring/management system, and its reliability is vital for the effectiveness of the system. Magnetic sensors

are largely used in this step for their relevance and high coverage in vehicle detection. All current systems use detection algorithms that rely on the regularity of magnetic signature. While this may be ensured by some magnetic sensors, it is not for many others. The contribution in this paper is to tackle this problem and propose a new vehicle monitoring solution based on a detection algorithm that works for sensors with irregular signatures. The proposed algorithm is based on processing the magnetic signal and thoroughly analyzing the number/direction of oscillations. This enables to detect vehicles with different shapes of signatures and makes the algorithm effective with all type of magnetic sensors. The proposed algorithm has been implemented on MICAz sensor motes and tested in real world scenario. Experimentation results confirm the effectiveness of the proposed algorithm, with more than 93% of reliability.

REFERENCES

- [1] S.-Y. Cheung and P. Varaiya, "Traffic surveillance by wireless sensor networks: Final report california path research report," Institute of Transportation Studies, University of California at Berkeley, Tech. Rep., 2007.
- [2] S. Yuan and H. Schumacher, "Vehicle microwave radar system for 2D and 3D environment mapping," in IEEE MTT-S International Conference on Microwaves for Intelligent Mobility (ICMIM), 2015.
- [3] E. Belyaev, A. V. Vinel, A. Surak, M. Gabbouj, M. Jonsson, and K. O. Egiazarian, "Robust vehicle-to-infrastructure video transmission for road surveillance applications," IEEE T. Vehicular Technology, vol.64, no. 7, pp. 2991-3003, 2015.
- [4] E. Sifuentes, O. Casas, and R. Pallas-Areny, "Wireless magnetic sensor node for vehicle detection with optical wake-up," IEEE Sensors Journal, vol. 11, no. 8, pp. 1669-1676, 2011.
- [5] E. Karbab, D. Djenouri, S. Boulkaboul, and A. Bagula, "Car park management with networked wireless sensors and active RFID," in IEEE Int Conference on Electro/Information Technology, May 2015, pp. 373-378.
- [6] T. M. Kwon and R. Weidemann, "Portable cellular wireless mesh sensor network for vehicle tracking in an intersection, research report," Center for Transportation Studies, University of Minnesota, Tech. Rep., 2008.
- [7] S. Cheung, S. Coleri, B. Dundar, S. Ganesh, C. Tan, and P. Varaiya, "Traffic measurement and vehicle classification with a single magnetic sensor," Journal of Transportation Research Record, vol. 1917, p. 173181, 2005.
- [8] Q. Wang, J. Zheng, B. Xu, and Y. Huang, "Analysis and experiments of vehicle detection with magnetic sensors in urban environments," in IEEE International Conference on Cyber Technology in Automation, Control, and Intelligent Systems (CYBER), 2015.
- [9] M. Najim, Digital Filters Design for Signal and Image Processing. Wiley, 2010.